

PARSEC'S ASTROMETRY DIRECT APPROACHES

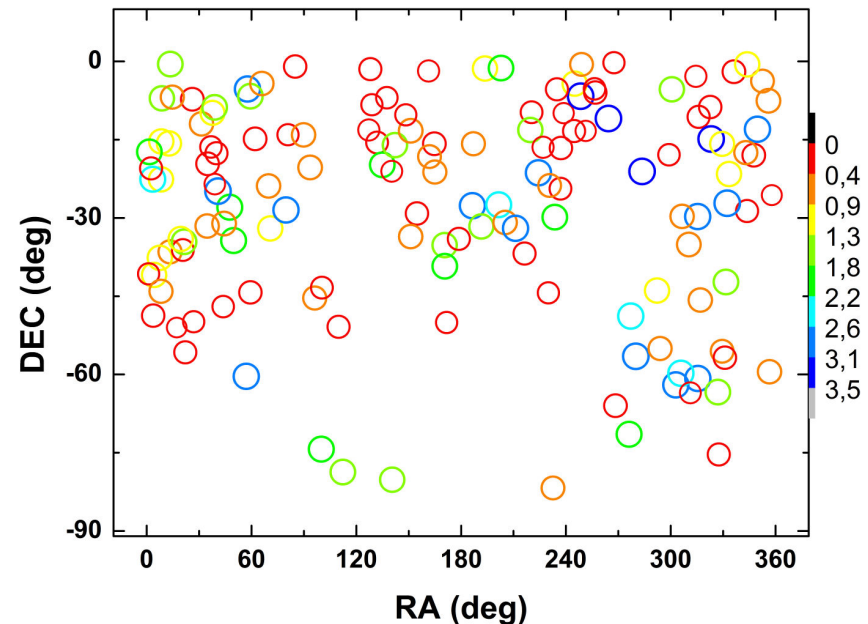
**A.H. ANDREI -- Observatório Nacional - ON/MCTI, Brasil
Osservatorio Astronomico di Torino – OATo/INAF, Italy
Observatoire de Paris – SYRTE/OP, France
Observatório do Valongo – OV/UFRJ, Brasil**

Parallaxes - and hence the fundamental establishment of stellar distances - rank among the oldest, keyest, and hardest of astronomical determinations. Arguably amongst the most essential too. The direct approach to obtain trigonometric parallaxes, using a constrained set of equations to derive positions, proper motions, and parallaxes, has been labeled as risky. Properly so, because the axis of the parallactic apparent ellipse is smaller than one arcsec even for the nearest stars, and just a fraction of its perimeter can be followed. Thus the classical approach is of linearizing the description by locking the solution to a set of precise positions of the Earth at the instants of observation, rather than to the dynamics of its orbit, and of adopting a close examination of the never many points available. In the PARSEC program the parallaxes of 143 brown dwarfs were aimed at. Five years of observation of the fields were taken with the WIFI camera at the ESO 2.2m telescope, in Chile. The goal is to provide a statistically significant number of trigonometric parallaxes to BD sub-classes from L0 to T7. Taking advantage of the large, regularly spaced, quantity of observations, here we take the risky approach to fit an ellipse in ecliptical observed coordinates and derive the parallaxes. We also combine the solutions from different centroiding methods, widely proven in prior astrometric investigations. As each of those methods assess diverse properties of the PSFs, they are taken as independent measurements, and combined into a weighted least-square general solution. The results obtained compare well with the literature and with the classical approach.

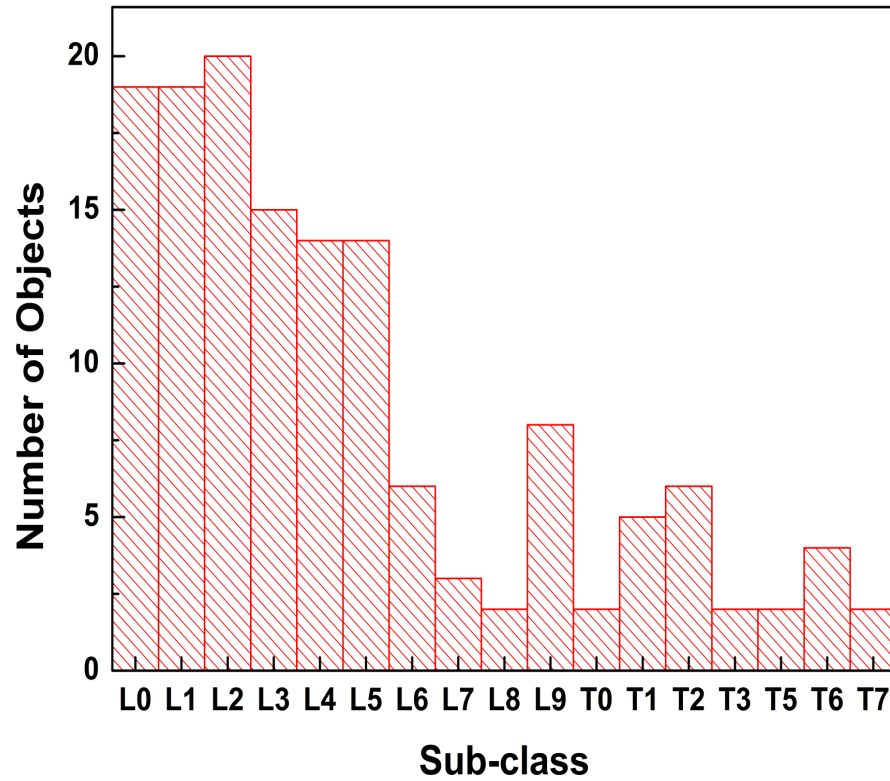
This work belongs to all participants of PARSEC project

PARSEC at a glance

- measures parallaxes of 120 L and 23 T dwarfs brighter than $z=20$ in the southern hemisphere
(most of these objects will not be observed by GAIA)
- using WFI on the ESO 2.2m, in the z band (compromise between optimal QE in I band and target typical brightness ($I-z \sim 2$))
- started in 2007 and ended on early 2011, 4-6 epochs/year (Brasil-Italia cooperation which evolved to the IPERCOOL/BR-IT-UK-CN consortium)

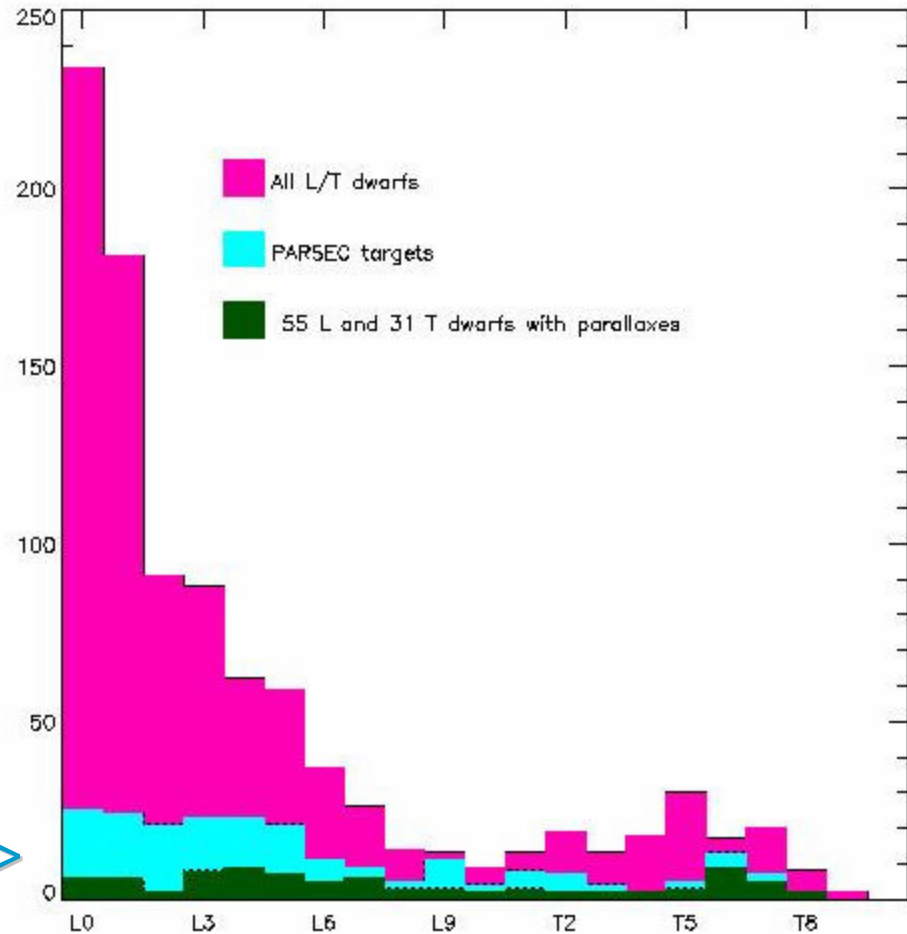


PARSEC Targets by sub-class



PARSEC Targets ->

Catalogue data from
www.dwarfarchives.org

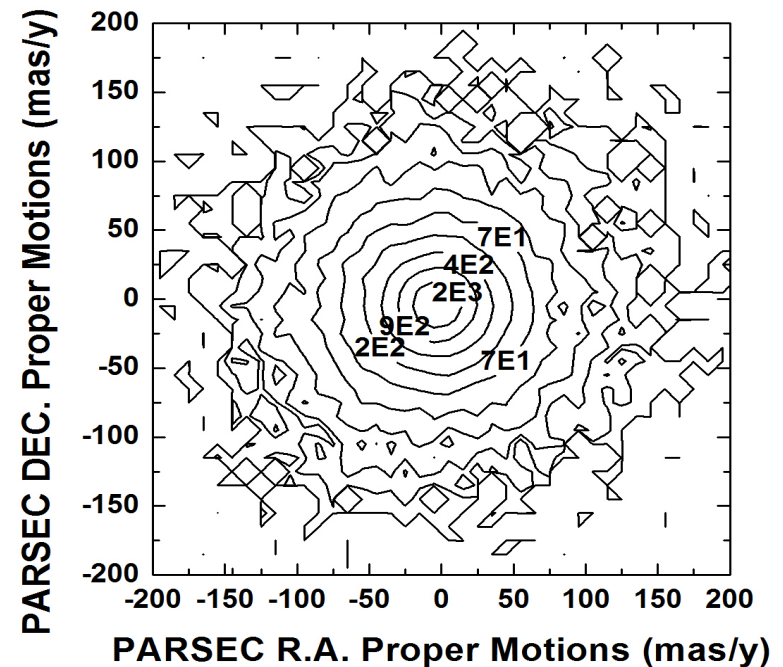
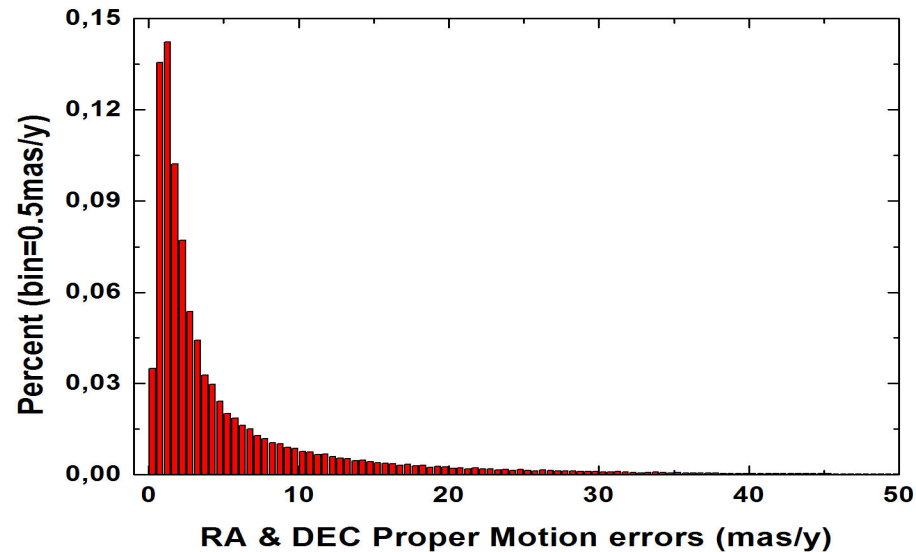


Main Output

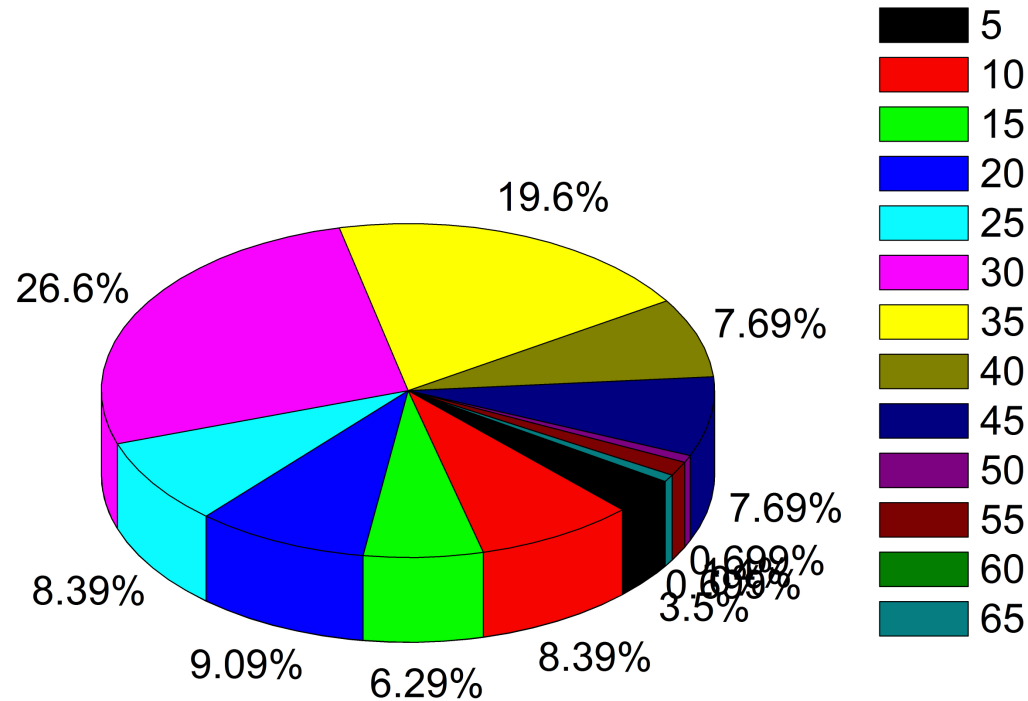
- **More than 100% increase of L dwarfs with trigonometric parallaxes**
- **Increment to at least 10 (in conjunction with published results) the number of objects per spectral sub-class in the range L0 to T7**
- **Study the binarity fraction of brown dwarfs**
- **Single out interesting/benchmark objects for extended spectroscopic observation**

Additional Outputs

- Proper motion catalogue of 197,500 2MASS stars on the 140 ~ 0.3 sq.deg fields using positions PARSEC for the second epoch
- independent validation of UCAC2 proper motions
- search for fast-moving objects
- search for stellar companions
- brown dwarf candidate selection tool



Full Program observation map



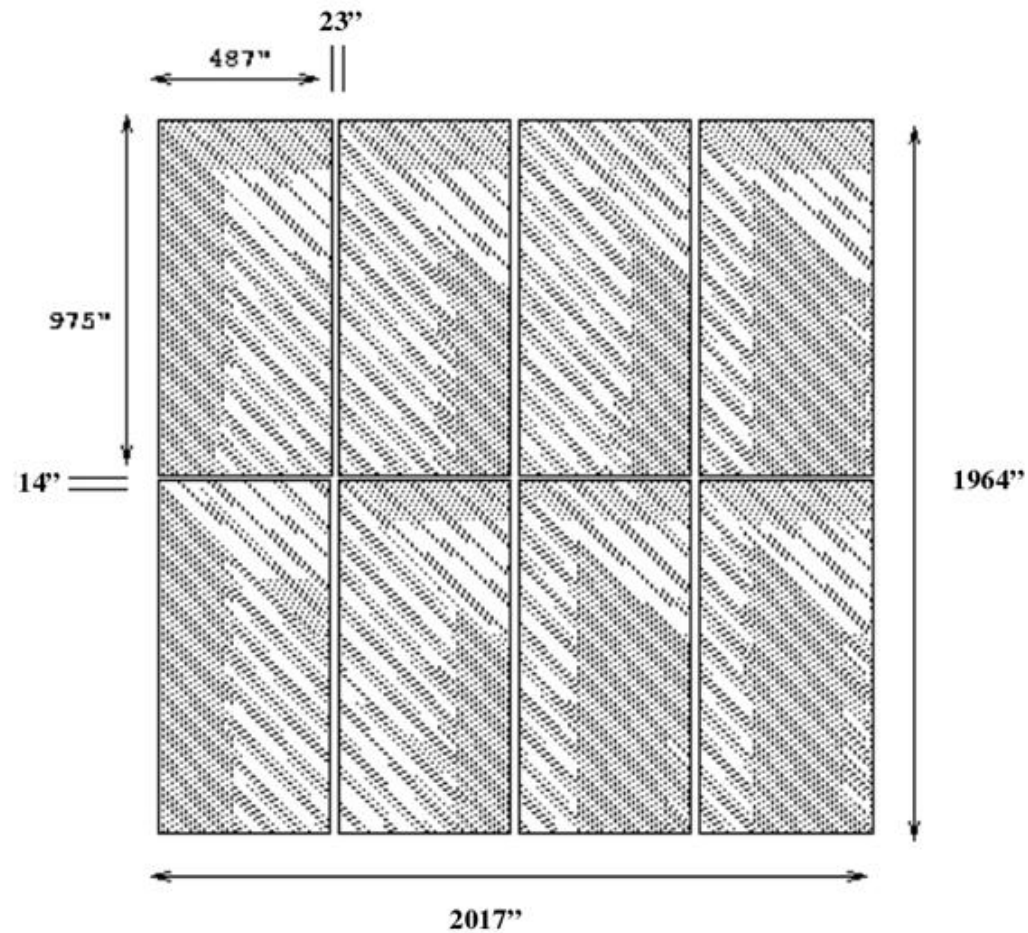
- Out of the 143 targets, just 4 were observed around only 1 revolution; and 9 around 2 revolutions.

- From L0 to T7 no sub-class had more than 1 element with observations within only 1 revolution.

- The color scheme indicates the number of observations. On the edge of the slices are the percent of sources observed those many times..

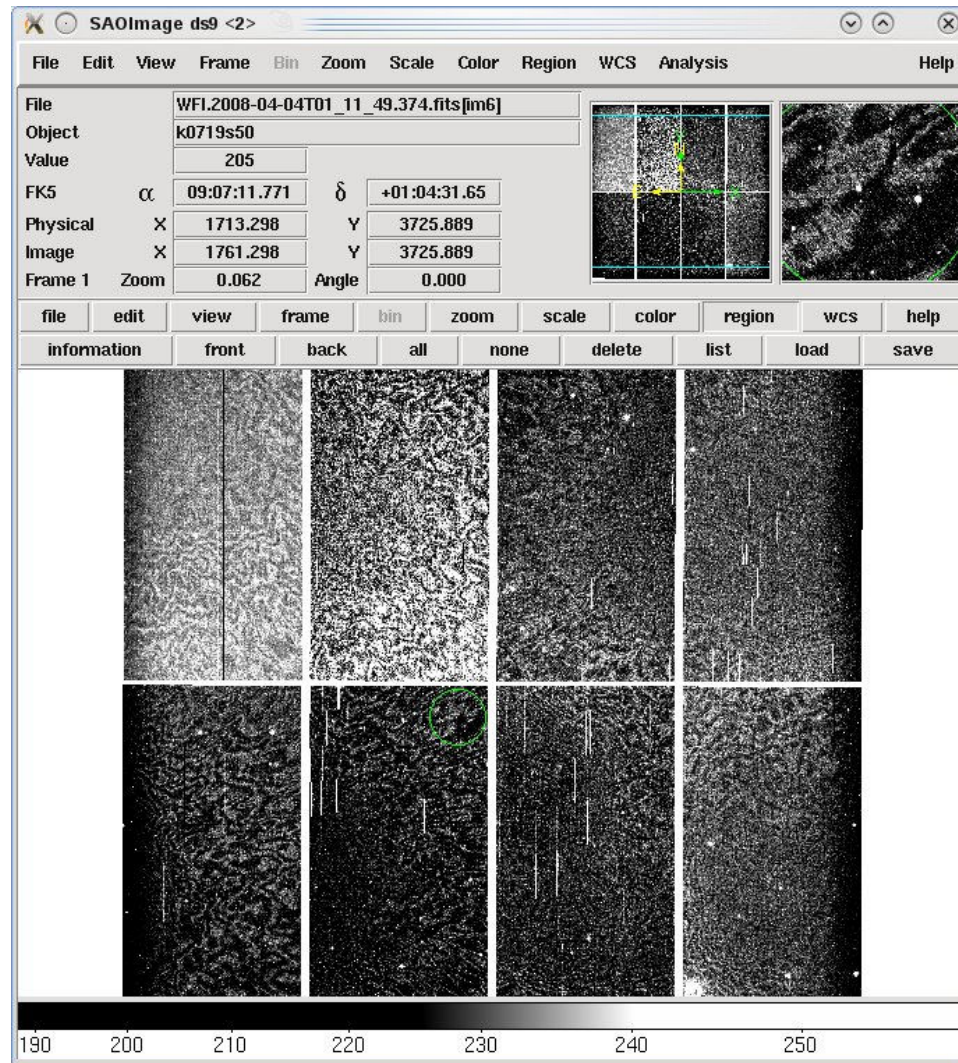
Main Output

- **More than 100% increase of L dwarfs with trigonometric parallaxes**
✓ checked - preliminary parallaxes for all targets with observations spread over 3 or more years, and at least 2 independent points of the parallactic ellipse in each year - totaling 95 parallax determinations.
- **Increment to at least 10 (in conjunction with published results) the number of objects per spectral sub-class in the range L0 to T7**
✓ checked - no sub-class remained underrepresented.
- **Study the binarity fraction of brown dwarfs**
✓ checked - two targets examined; a IPERCOOL task force will fully address the issue for the whole program.
- **Single out interesting/benchmark objects for extended spectroscopic observation**
✓ checked - SOAR spectroscopy follow-up program running its 2nd year, to more than 50 targets examined.



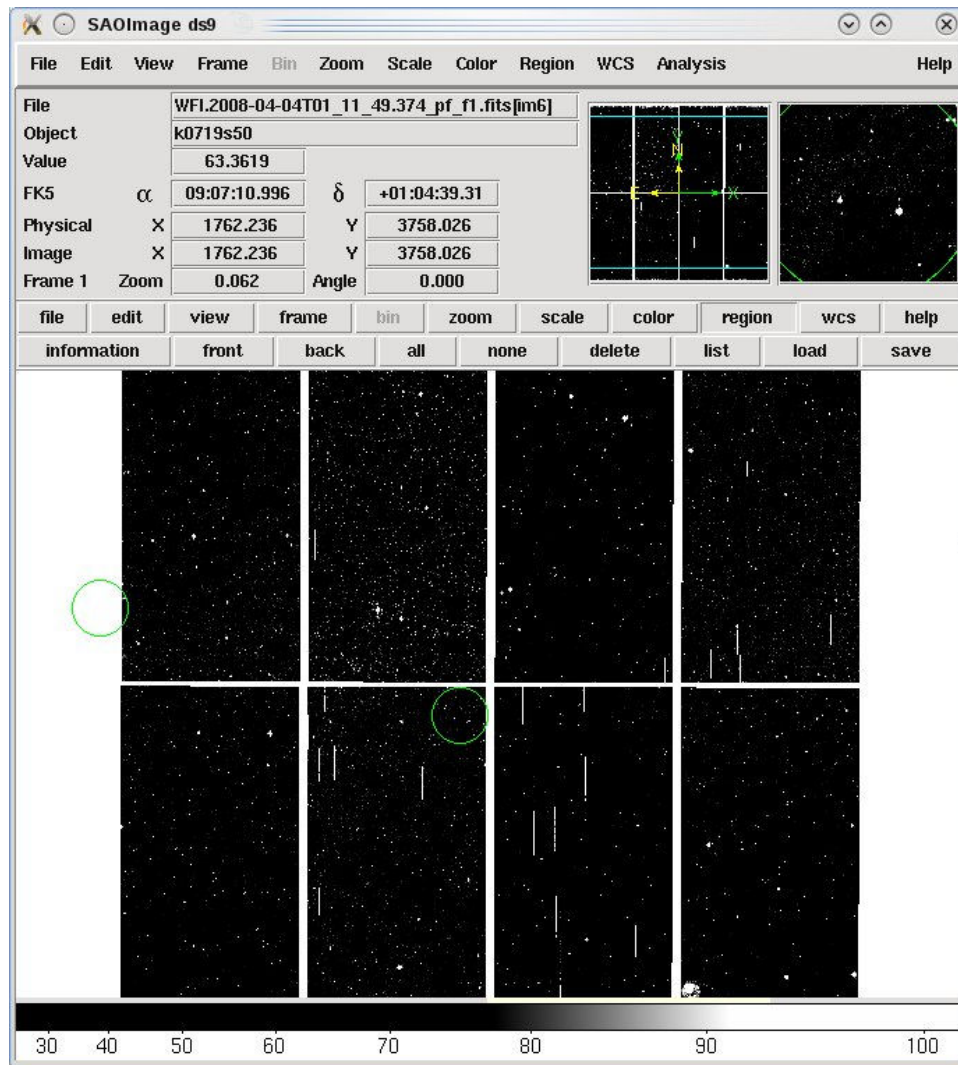
Coverage: $0.56 \times 0.54 \text{ deg}^2$ (0.238 "/pix)

- ESO 2p2 WFI camera geometry, field, and pixel scale. The target always sit in CCD#7, nearby the optical axis.



- The WFI has significant astrometric distortions but **stability** and **repeatability** the only crucial requirements for relative astrometry

- Raw image of a typical observation. The target's spot is highlighted on the upper-left corner of CCD#7. Notice the heavy fringe pattern (due to the z-band).



- For parallax determinations always only the top third of CCD#7 is used.

- This leads to less distortions, and further minimizes the DCR correction, which is already negligible in the z band.

- Corresponding cleaned image. Flat, bias, and a nightly fringe map correction applied. The white dots are real stars, that were hidden in the noise of the raw image.

Image Treatment

The initial image treatment uses standard IRAF routines for bias and flat. However fringe removal required a tailored approach. **The interference fringes in the infrared band images are severe, an examination of the counts shows they can vary by up to 10% over the distance of a few pixels.** Fringing is an additive effect that can be corrected making a fringe map and subtracting it from the raw images. The suggested approach is to apply a standard fringe map which is updated at periodic intervals. We found it improved our centroiding by adopting a different approach and to understand why we first consider the cause of fringing. Fringes are caused by the constructive and destructive interference of the night sky emission lines that are reflected from the bottom of the CCD silicon layer with incoming radiation. **Fringes are time and observation dependent** for a number of reasons e.g.: changes in the brightness of the night sky emission lines, changes in the thickness of the silicon layer which is a function of the temperature of the CCD, changes in the angle of incidence of the light on the CCD which is a function of flexure. **The ideal case would therefore be to make a fringe map for each image but this is not feasible. Our compromise is to make a nightly fringe map whenever possible. The general procedure to construct a fringe map is to mask out objects then build a mean map from all of the observations in a given night scaled appropriately to reveal the fringe signal.**

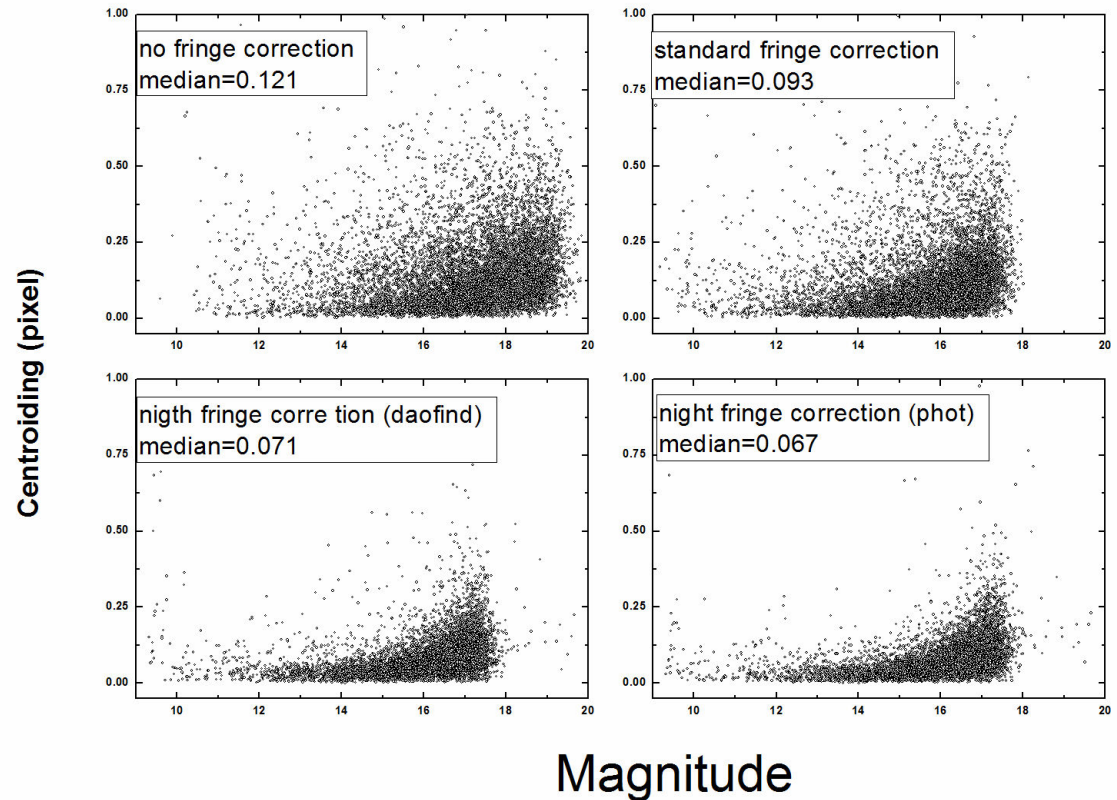
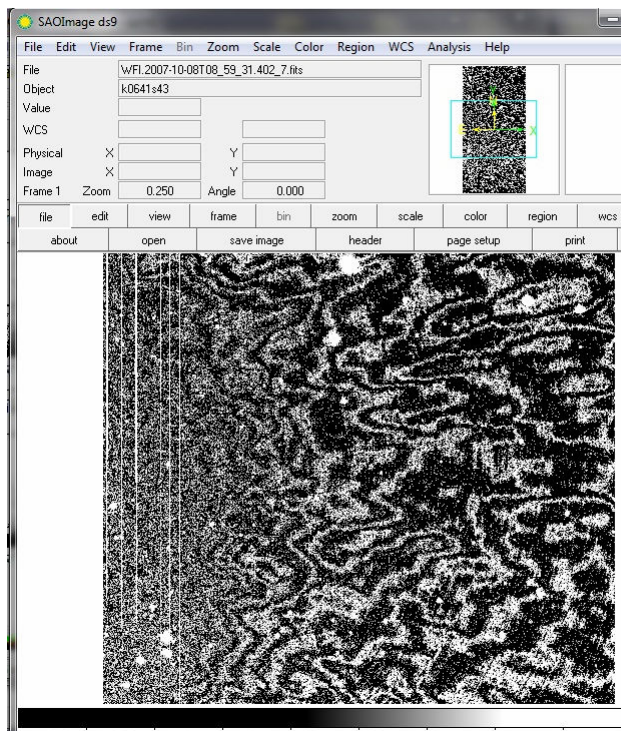
Image Treatment

Specifically we followed the following steps:

1. For all images we identify all the objects and make an object mask.
2. For each image we make a sky map by fitting a plane to all the unmasked pixels including a 3 clipping rejection criteria. This changes in the course of the night so it is necessary to remove it from each frame independently.
3. We select a fringe calibration image subset consisting of all the short 50s and 4 of the long science exposures. We did not include all the science images in this subset as the object mask does not always cleanly block out all of the target signal and using all the science frames with the target on the same pixel results in a ghost image around the move-to-pixel position.
4. We make a median image by scaling all subset images by the exposure time and making a median of the unmasked pixels.
5. The first fringe map is constructed by smoothing the median image using a block size of 5 pixels.
6. This first fringe is subtracted from all images providing sky subtracted and relatively fringe free observations.
7. We make a new median image scaling the cleaned subset images by the weighted mean difference between the input image and the fringe image.
8. We construct a new fringe map smoothing the median image and then apply it to all the cleaned images providing fringe-free images.

Image Treatment at a glance

- Image treatment with standard IRAF routines, but fringing removal with tailored approach.
- Variation of counts as high as 10% over the distance of few pixels are cured by generating a **nightly fringe map** built from the science frames and subtracted from each **raw frame** in two passes.
- First, the image contribution is scaled using the **exposure time**.
- Next, the **image mean counts** are used as scale factor.



Astrometric Solution

- The former solutions (Andrei et al., 2011, 2013) used respectively the UCAC2 and UCAC4 as base catalogs.
- **Both fully cover the south celestial hemisphere, for R magnitudes of about 7.5 to 16, resulting on an average star density of 0.76 star per square arc-minute.** The observed positional errors are about 20 mas for the stars in the 10 to 14 magnitude range, and about 70 mas at the limiting magnitude of $R \sim 16$.
- For the current solution the PPMXL is employed as base catalog. This is done both to substantially multiply the number of reference stars, as well as for practical reasons due to matching difficulties between the various centroid solutions available.
- The PPMXL is a catalog of positions, proper motions, 2MASS and optical photometry of 900 million stars, aiming to be complete down to about $V=20$ full-sky. **The resulting average stellar density is 6.06 stars per square arc-minute. The mean errors of positions at epoch 2000.0 are 80 to 120 mas, if 2MASS astrometry could be used, 150 to 300 mas else.**
- The following table of observed-minus-calculated (OC) averages shows that there is no loss for the astrometric solution by adopting the PPMXL.

Astrometric Solution

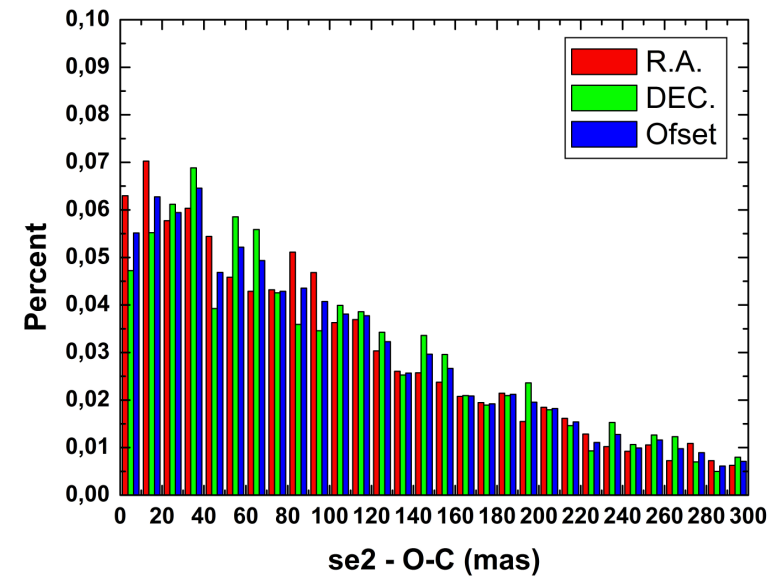
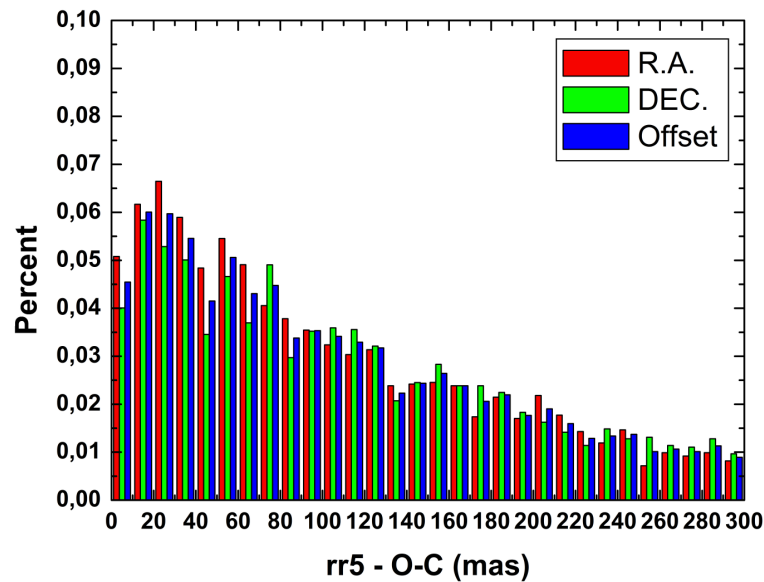
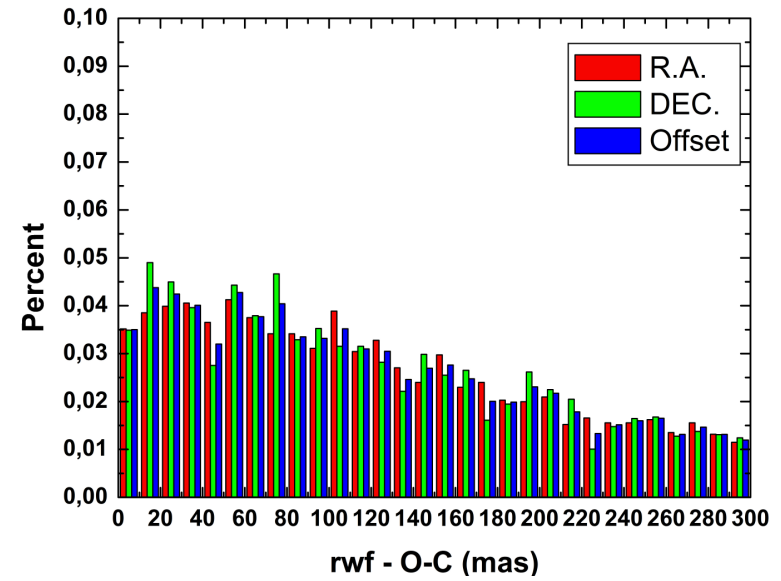
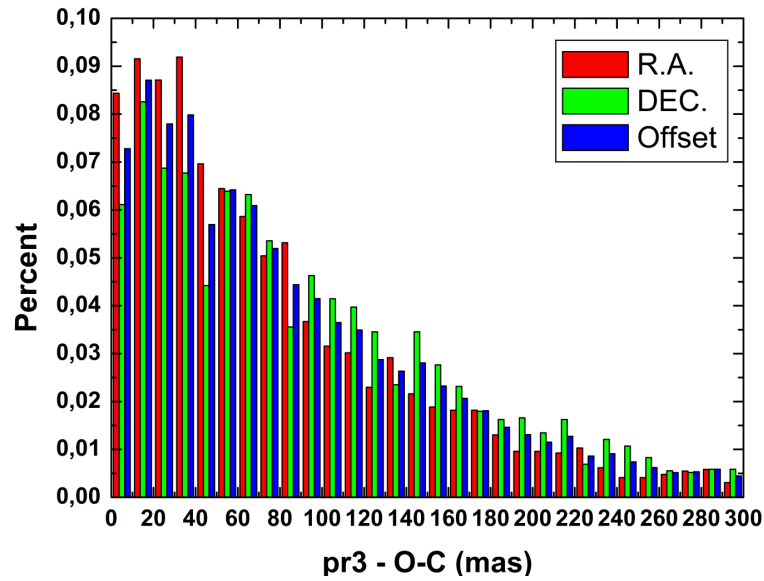
Catalog	Solution	$ \Delta\alpha\cos\delta $ (mas)	$E(\alpha)$	$ \Delta\delta $ (mas)	$E(\delta)$	$ \Delta $ (mas)	$E(\Delta)$
UCAC	phot	152.5	16.1	151.2	15.9	151.9	16.0
PPMXL	pr3	91.9	10.3	109.3	10.9	100.6	10.7
PPMXL	rwf	148.0	15.6	178.4	17.8	163.1	17.2
PPMXL	rr5	196.8	18.4	189.7	18.0	193.3	18.2
PPMXL	se2	134.8	14.3	139.7	14.3	137.3	14.3

Astrometric Solution - centroiding

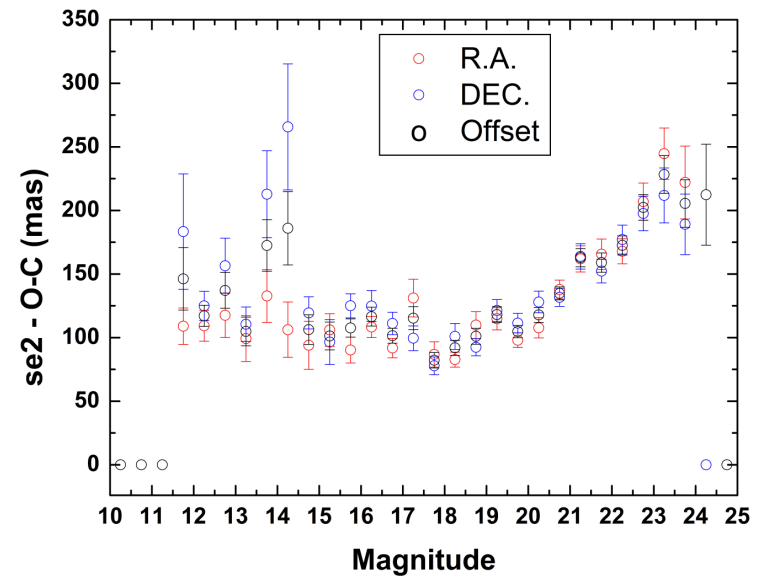
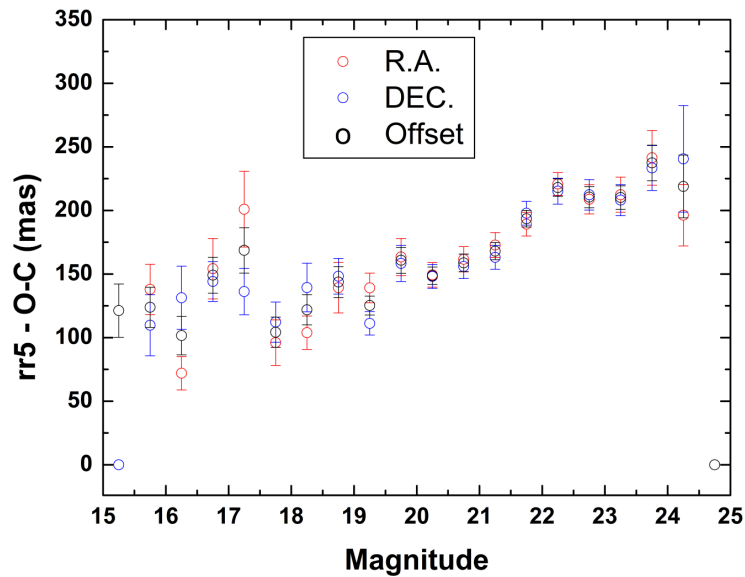
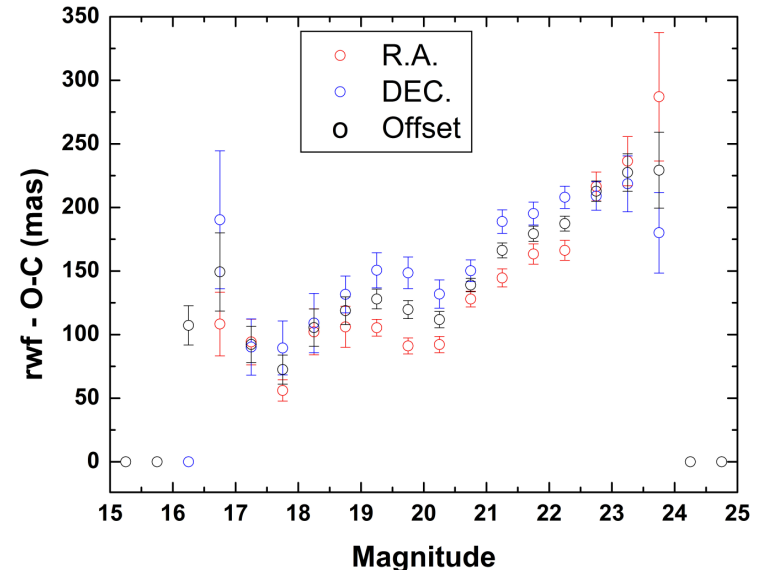
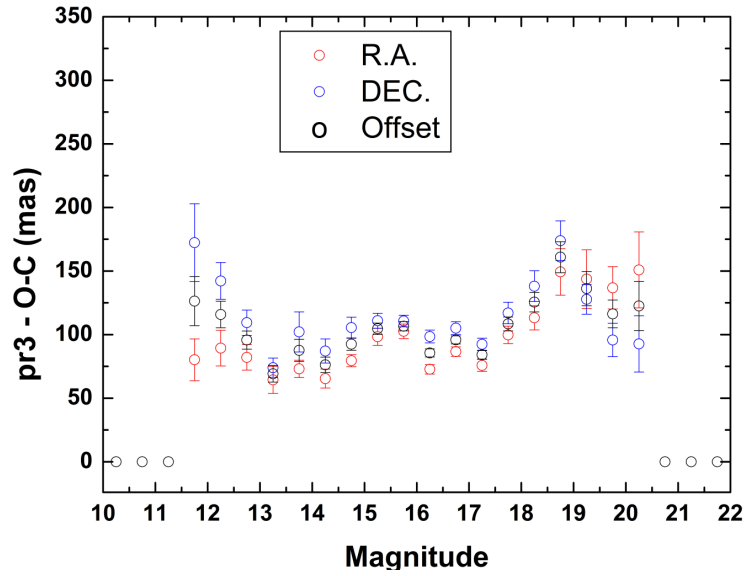
Catalog	Solution	$ \Delta\alpha\cos\delta $ (mas)	$E(\alpha)$	$ \Delta\delta $ (mas)	$E(\delta)$	$ \Delta $ (mas)	$E(\Delta)$
UCAC	phot	152.5	16.1	151.2	15.9	151.9	16.0
PPMXL	pr3	91.9	10.3	109.3	10.9	100.6	10.7
PPMXL	rwf	148.0	15.6	178.4	17.8	163.1	17.2
PPMXL	rr5	196.8	18.4	189.7	18.0	193.3	18.2
PPMXL	se2	134.8	14.3	139.7	14.3	137.3	14.3

- **phot** – from IRAF: enhanced centroid task.
- **pr3** – from GBOT: astrometry driven; wings and skewness are taken into account through an initial determination of the centroid by marginal X,Y projections. baricenter performed on a tight rectangular window.
- **rwf** – from CASU: photometry driven; 2 sequential steps of local background removal; initial clipping run to un-weight pixels with discrepant counts; baricenter finally applied; 2D regular, linear fitting-apt components of the image are accessed.
- **rr5** – from TOPP: astrometry driven; unweighted bi-dimensional gaussian fit, although assign zero weight to pixels which count approached the CCD nominal saturation limit; psf model dominates.
- **se2** – from SEXTRACTOR: astrometry driven; baricenter performed over a gaussian defined window; summation performed relatively to the spatial minima, skewness and large wings are assumed constant over the astrometry field or of minor importance, as such the peak is well determined.

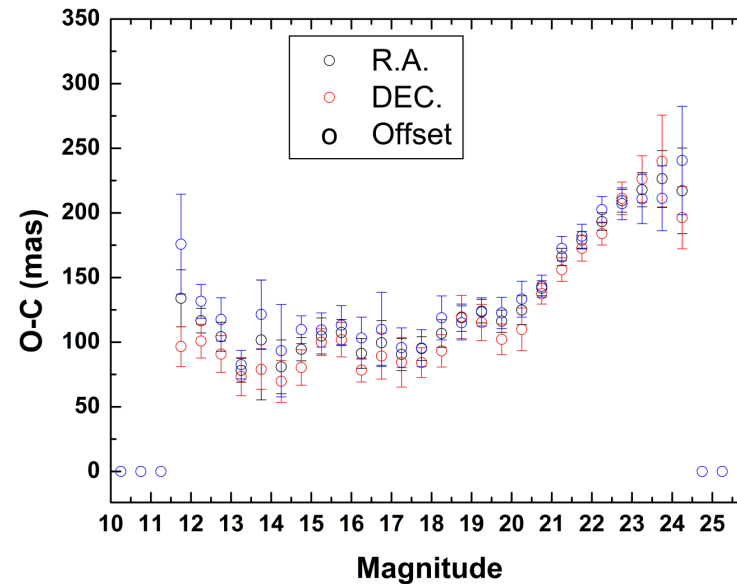
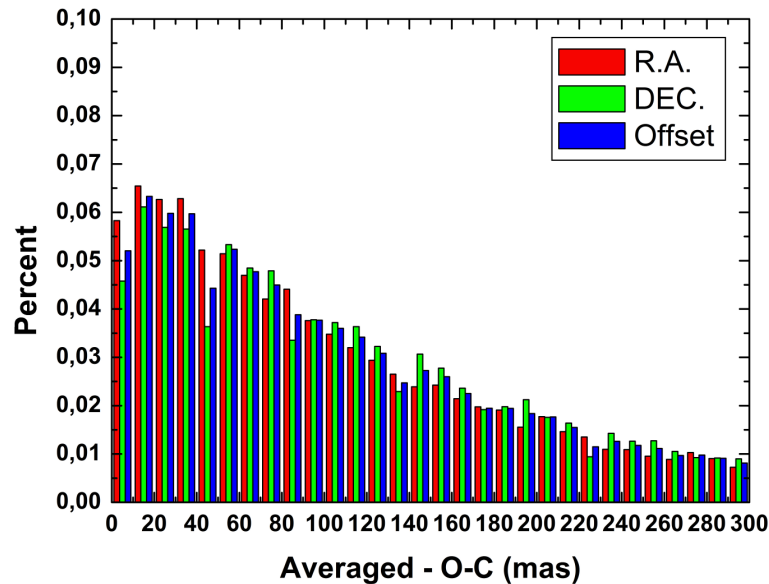
Astrometric Solution - centroiding



Astrometric Solution - centroiding



Astrometric Solution - adopted average centroid



- Considering that:
- The four centroidings obtained have previously refereed methodology discussion and astrometric applications;
- Also on our sample the four centroidings offer comparable astrometric results;
- The four centroidings define each one conceptually different and independent assessment of the centers of any given star, at any given magnitude, any given state of the detector sensitivity, and at any given sky condition;
- Our results are obtained by averaging the solutions coming from the four independent measufrements – **of the same observations.**

Objects Matching

Matching – The probability of correct matching of one object in two frames is $P = 1/(\Phi S)$, where Φ is the stellar density and S is the frame size.

Usual cone search strategies run into trouble for long time intervals. We avoided such pitfalls by adopting the following strategy:

1. because of moving-to-pixel telescope pointing and double exposures, unpaired objects are assigned low order in the matching process.
 2. assigning high order in the matching process to objects with no proper motion between the first two nights.
 3. using relative astrometry precise to better than 100mas, under those conditions P is larger than 0.99 already when the third night is added even for $\Phi=1000/\text{deg}^2$.
 4. removing the stars matched in the previous step Φ drops dramatically, and the process re-starts taking stars with smallest proper motions.
 5. finally the objects unpaired in the first step, and cases of suspicious magnitude or position matching are considered, now allowing for periodical jitter.
- The pipeline converges rapidly, has shown to be robust during artificial and surveyed tests, and is effective to sign out binary candidates.

Objects Matching

Fitting – **Before start the matching process all frames must be placed onto a common reference frame.** Instead of the usual choice by the first or densest frame as reference we opted to build a mean frame. The mean frame is build by step-wise polynomial adjustment of time close frames. **We simulated the observation of a patch of the sky observed twice along 26 nights with up to 800 stars, mimicking a typical PARSEC set.** Using a gaussian noise generator stars appeared or not in each frame, centroid errors were assigned, plus terms of tilt and telescope pointing. **The table below summarizes the results obtained taking as reference frame either the first frame of the sample, or the densest, or finally the mean frame – which is clearly the optimal choice.** The building of the mean frame, though asking for an additional computational effort, saves steps when later matching the objects.

Solution	Stars Matched	Mean Precision (mas)
1st frame	257 ± 76	0.0028
Densest frame	493 ± 128	0.0026
Mean frame	527 ± 134	0.0023

Parallaxes - Direct ellipse fitting

- As the starting point a mean frame is build using the step-wise polynomial adjustment of time close frames and the matching by hierarchical cone search.
- Next the ecliptic standard coordinates (ξ'_i, η'_i) at t_i epoch of observation of the target star are derived.
- Hence (ξ'_i, η'_i) can be fitted with an elliptic motion modeling the parallactic effect superimposed to a linear term which accounts for the star's transversal motion as

$$\xi_{t_i}(x, y) = \pi_\xi \sin(t_i + \phi_\xi) + \mu_\xi(t_i - t_0)$$

- Above, π_ξ is the target's parallax, Φ_ξ is a phase term, μ_ξ is the longitudinal proper motion and t_0 the epoch of the mean frame. And analogously for the η' component.
- The effect of Earth's eccentricity is disregarded, given the typical distances of our targets. It can be in principle computed and corrected for being a purely geometrical effect. Nevertheless a computation of the differences for 3 fictitious stars at 20pc, and with ecliptic latitude $b= 0^\circ, 45^\circ, 90^\circ$, sampled from 4 to 9 times along 6 months covering the span of the year (or of ecliptic longitudes), adjusted to a "parallactic" ellipse shows no contribution larger than 10×10^{-8} arcsec to the parallax.

Parallaxes - Results

- As an example, we report the reduction of 6 years of observations (93 frames, 54 reference stars) of the high proper motion star LHS3482 (2MASS J19462386+3201021) with the three techniques giving very consistent results, as shown in Table.
- It can be noted that the quoted errors are sensibly smaller in the case of the direct method. An explanation could lie in the fact the standard deviations coming from the covariance matrix are slightly underestimated, while in the other two cases, the errors are estimated from the residuals of the fit to the target's trajectory and could be more realistic indicators of the true errors.

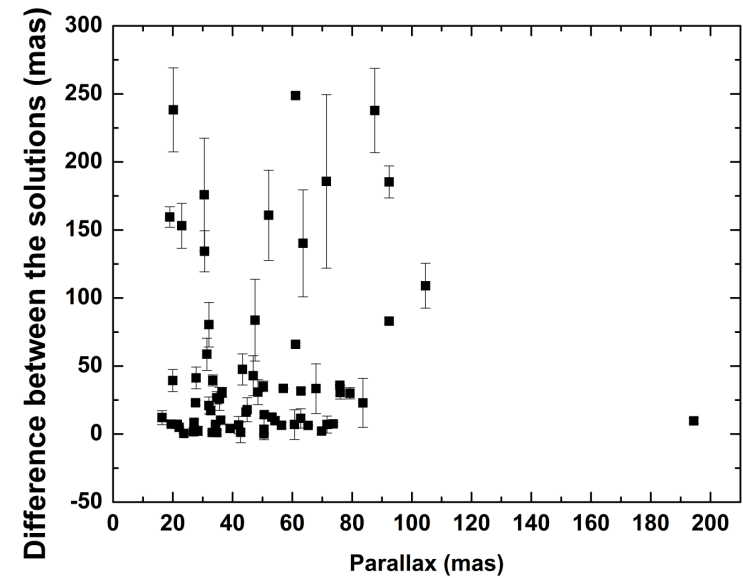
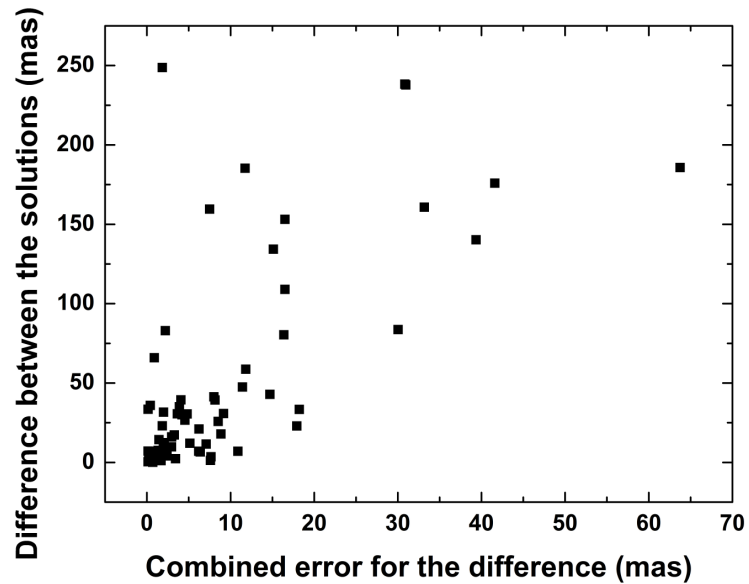
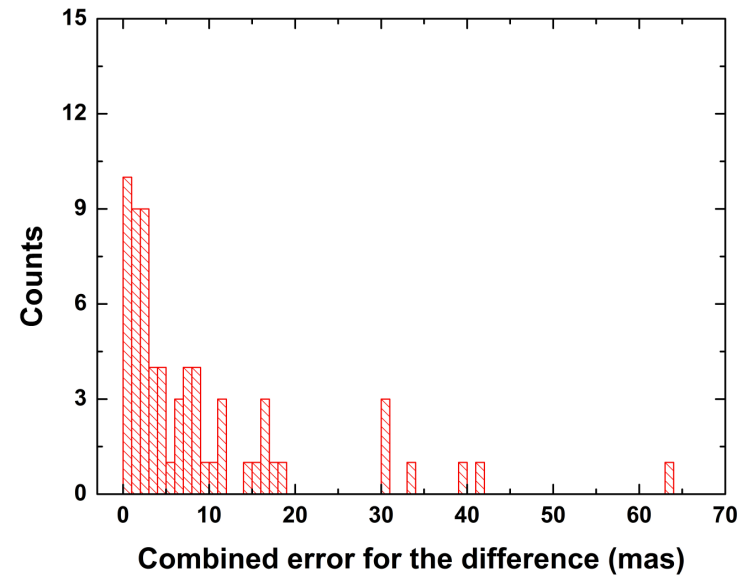
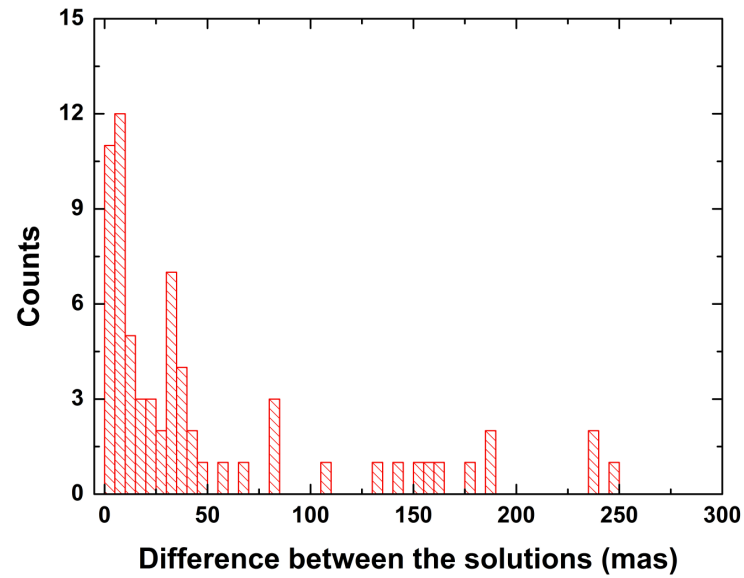
Method	π (mas)	$\mu_{\alpha} \cos\delta$ (mas/y)	μ_{δ} (mas/y)
Block iterative	68.7 ± 4.0	458.8 ± 1.2	-391.2 ± 2.0
Direct LS	68.9 ± 0.8	457.5 ± 0.2	-390.4 ± 0.3
Ellipse fit	70.0 ± 3.2	467.7 ± 0.7	-392.0 ± 1.7

Parallaxes - Results, the careful formulation

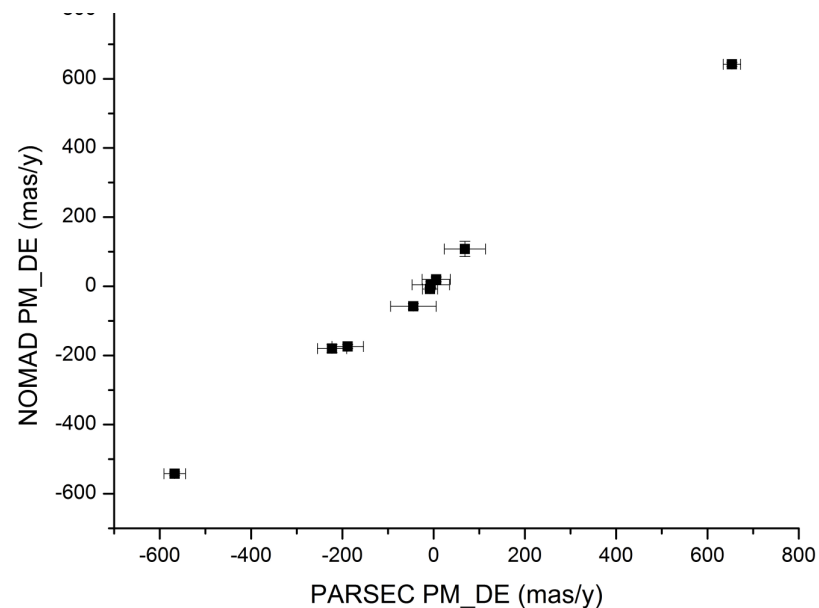
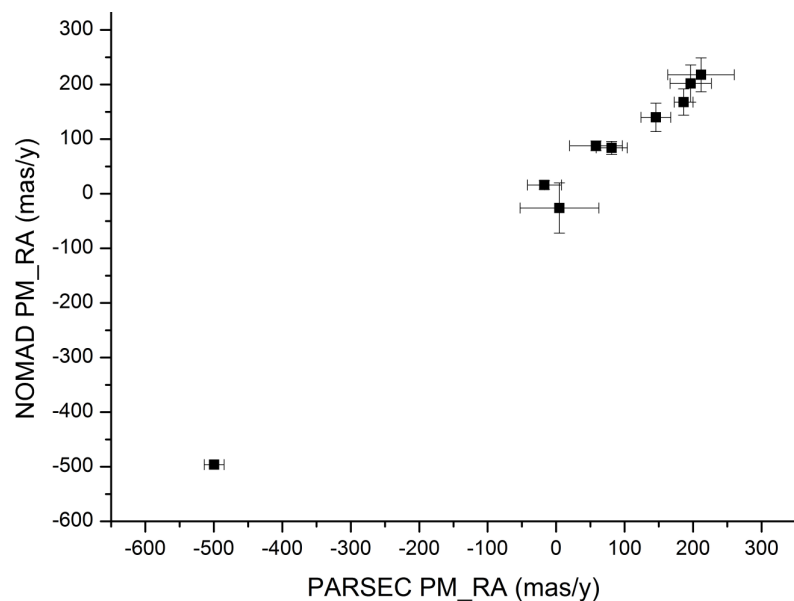
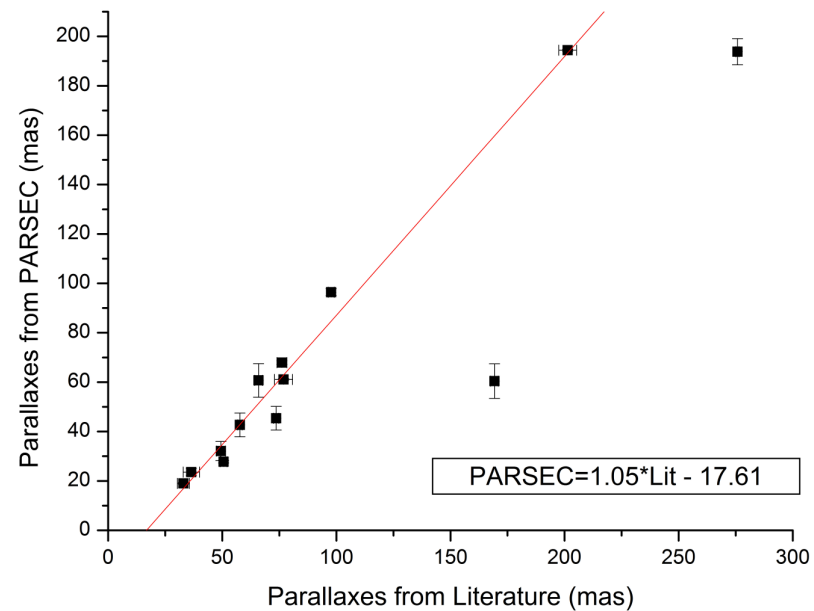
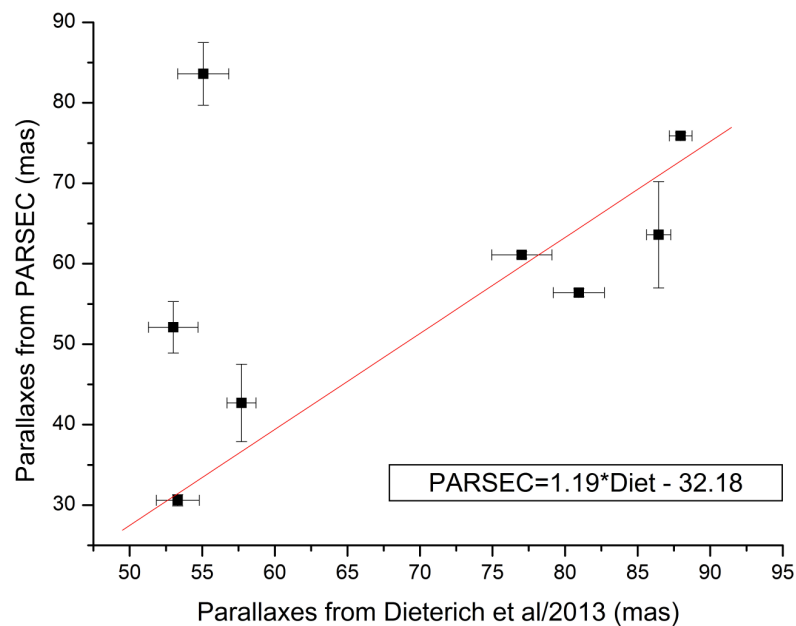
- Improvements on the general ellipse fitting solution:
 - 1- exact observation time, obliquity, and eccentricity.
 - 2- exact ecliptic longitude.
 - 3- numerical (exact, using the Newton's chords*) solution for the eccentric anomaly.
 - 4- exact coefficients for the terms of parallaxe in longitude and latitude (projection of Earth's orbit on the circle of latitude).
 - 5- tilt term to account for the angle between the apsides and the line of solstices.
 - 6- two free parameters to account for faulty mean position.
- The points (1) to (3) can contribute to less than 8mas (assuming a parallax as large as 1arcsec).
- The point (4) to (6) were already present before as free parameters of the general ellipse adjustment. Variation upon them would stretch the ellipse – unlikely variations of several arc-minutes would be required to create a milli-arcsec effect.

(*) acknowledgements to D.C. Andrei

Parallaxes - Results, the careful formulation



Parallaxes - Results, comparisons



Parallaxes - Results, the Table (as it is now)

Target	No	Ns	Parallax (tightness)		Parallax (completeness)		Parallax (quartiles)		P. M. -R. A.		P. M. -DEC.	
k0004s40	16	8	61.1	0.4	61.1	0.4	61.1	0.4	676.7	6.2	-1472.6	1.6
k0032s44	22	8	36.5	1.0	36.5	1.0	36.5	1.0	112.3	3.5	-67.9	2.4
k0058s06	22	8	26.7	0.1	83.8	7.6	128.8	6.6	145.0	2.6	-112.9	3.7
k0109s51	24	8	50.6	1.2	50.6	1.2	50.6	1.2	211.6	13.5	68.5	2.6
k0128s55	20	8	23.7	0.1	23.7	0.1	64.3	2.1	-231.9	13.3	86.1	13.7
k0147s49	22	8	21.8	0.1	21.5	0.1	21.8	0.1	-68.9	13.8	-276.6	13.2
k0205s11	24	8	66.6	0.1	27.8	0.5	39.5	0.8	434.8	1.2	52.1	2.2
k0227s16	14	8	33.4	1.7	33.4	1.7	36.6	1.5	422.9	5.4	-309.4	2.7
k0239s17	21	8	47.8	0.6	87.6	4.5	94.4	4.7	58.3	1.4	-94.0	2.3
k0255s47	14	8	194.4	0.4	194.4	0.4	194.4	0.4	999.2	3.9	-513.4	3.0
k0350s05	36	8	19.5	1.0	19.5	1.0	48.5	4.5	-31.6	1.7	26.7	2.1
k0357s44	20	8	22.1	0.4	22.1	0.4	24.4	0.4	95.0	15.0	0.4	16.1
k0408s14	27	8	34.3	0.3	34.3	0.3	42.0	0.8	210.6	1.5	-94.9	1.5
k0423s04	29	8	91.1	4.9	60.7	6.8	80.1	6.5	-277.4	2.8	100.2	1.1
k0439s23	28	8	69.8	0.4	69.8	0.4	71.3	0.5	-130.6	3.8	-150.2	1.7
k0518s28	35	8	54.2	1.4	54.2	1.4	54.2	1.4	-99.2	2.2	-260.3	5.5
k0523s14	30	8	56.4	0.5	56.4	0.5	58.8	0.4	107.0	5.7	147.1	13.6
k0539s00	29	8	67.9	0.8	67.9	0.8	67.9	0.8	130.6	1.7	306.7	5.1
k0559s14	39	8	-999.9	-999.9	96.4	1.4	97.3	1.3	575.5	2.5	-355.8	6.7
k0624s45	37	8	34.7	0.1	34.7	0.1	34.7	0.1	-47.5	1.8	393.9	1.4
k0639s74	32	8	73.7	0.6	73.7	0.6	71.6	0.6	33.9	20.1	250.5	9.8
k0641s43	38	8	50.5	0.1	50.5	0.1	50.5	0.1	186.2	13.4	653.5	5.3
k0719s50	52	8	39.2	1.6	39.2	1.6	39.7	1.6	196.5	6.2	-44.5	5.3
k0729s78	54	8	27.1	2.1	27.1	2.1	27.7	2.1	-193.6	3.5	325.4	5.5
k0828s13	52	8	75.9	0.4	75.9	0.4	74.7	0.4	-591.1	13.1	18.1	14.3
k0832s01	43	8	63.9	1.6	62.9	1.6	63.5	1.6	69.2	13.7	-1.9	15.2
k0835s08	41	8	80.1	0.1	92.4	2.2	93.3	1.8	-510.5	6.4	288.3	1.1
k0859s19	49	8	76.0	4.6	76.0	4.6	77.6	4.7	-317.6	8.0	-133.9	9.1
k0921s21	49	8	71.6	1.9	71.6	1.9	66.4	0.1	257.3	6.3	-920.7	5.6
k0922s80	34	8	65.3	0.1	65.3	0.1	65.3	0.1	-44.0	4.9	101.2	21.0
k0928s16	40	8	26.9	0.2	26.9	0.2	34.1	0.5	-159.8	6.7	20.6	5.8
k0953s10	39	8	33.2	1.1	33.2	1.1	35.4	1.1	-111.2	13.5	-44.5	6.5

Parallaxes - Results, the Table (as it is now)

Target	No	Ns	Parallax (tightness)		Parallax (completeness)		Parallax (quartiles)		P.M.-R.A.		P.M.-DEC.	
k1004s13	30	8	57.0	0.1	57.0	0.1	57.0	0.1	-129.3	1.2	-209.4	2.8
k1004s33	32	8	-999.9	-999.9	49.3	0.9	49.4	0.9	321.5	7.9	-361.5	2.0
k1018s29	34	8	32.7	2.6	32.7	2.6	30.4	1.7	-369.9	6.0	-78.5	5.6
k1045s01	34	8	28.4	2.7	28.4	2.7	30.8	2.8	-499.6	12.7	-8.1	14.5
k1047s18	32	8	62.8	3.6	62.8	3.6	57.1	2.9	-353.4	1.2	41.1	5.4
k1058s15	30	8	42.7	4.8	42.7	4.8	38.0	0.9	-225.2	5.0	21.2	3.4
k1059s21	31	8	44.9	8.0	44.9	8.0	32.0	3.1	79.5	3.0	-122.6	4.9
k1122s35	29	8	37.4	4.8	46.9	5.1	56.0	6.0	-162.2	8.5	-282.2	2.4
k1122s39	25	8	-999.9	-999.9	41.1	5.9	39.7	4.2	51.8	2.7	-201.8	3.6
k1154s34	25	8	25.6	0.3	36.0	1.4	25.6	0.3	-175.8	3.1	27.4	1.1
k1228s15	25	8	32.1	3.9	32.1	3.9	40.8	2.5	143.7	2.8	-187.0	8.7
k1246s31	37	8	58.7	0.6	50.3	1.9	50.9	1.8	16.1	2.1	-562.3	3.9
k1326s27	37	8	83.3	2.3	71.4	6.7	71.4	6.7	-346.8	7.7	-21.7	1.1
k1341s30	28	8	34.7	2.5	34.7	2.5	39.3	1.2	5.0	5.0	-164.7	5.8
k1404s31	38	8	32.1	2.5	32.1	2.5	36.7	2.6	321.2	8.1	-12.3	9.1
k1425s36	38	8	89.9	0.5	63.6	6.6	89.9	0.5	-282.4	5.1	-466.9	5.0
k1438s13	57	8	54.1	9.7	139.6	36.9	42.1	6.9	130.1	6.8	-46.8	9.7
k1441s09	57	8	23.6	1.5	23.6	1.5	24.6	1.6	-197.4	8.6	-21.5	8.5
k1457s21	32	8	39.6	4.4	60.4	7.0	94.0	8.2	984.0	7.4	-1686.4	9.5
k1520s44	32	8	144.7	0.1	99.2	5.9	105.5	6.3	-630.5	7.2	-400.0	7.3
k1523s23	31	8	46.8	0.3	92.4	6.9	38.9	0.9	-162.7	1.2	-11.5	1.0
k1530s81	25	8	20.2	1.5	20.2	1.5	23.3	1.2	-587.2	12.8	-293.7	13.0
k1534s29	25	8	-999.9	-999.9	45.4	4.8	56.1	2.5	74.4	1.1	-260.7	8.7
k1539s05	34	8	-999.9	-999.9	54.3	0.1	54.3	0.1	577.1	8.8	137.6	5.9
k1547s24	34	8	91.8	0.1	82.8	6.4	91.8	0.1	-143.3	8.3	-129.5	7.3
k1548s16	32	8	35.5	9.2	79.5	18.0	73.4	16.4	-217.4	6.0	-115.9	7.2
k1618s13	34	8	23.0	0.1	23.0	0.1	23.0	0.1	-117.3	6.8	-85.8	6.7
k1620s04	34	8	19.0	0.3	19.0	0.3	19.0	0.3	-428.0	9.0	-19.3	2.8
k1633s06	31	8	30.6	0.7	30.6	0.7	30.4	0.7	-288.3	7.5	-231.7	9.5
k1636s00	33	8	20.0	1.5	20.0	1.5	21.6	0.9	-374.3	1.1	-220.8	1.2
k1645s13	35	8	13.5	1.7	50.5	6.2	44.7	5.9	-269.4	8.0	-597.3	16.3
k1705s05	38	8	83.6	3.9	83.6	3.9	94.1	1.9	108.1	8.2	-129.2	1.1

Parallaxes - Results, the Table (as it is now)

Target	No	Ns	Parallax (tightness)		Parallax (completeness)		Parallax (quartiles)		P.M.-R.A.		P.M.-DEC.	
k1707s05	39	8	50.4	0.6	79.3	4.2	52.4	0.8	126.0	6.4	8.2	14.5
k1737s10	58	8	45.1	2.6	45.1	2.6	54.4	3.4	4.2	14.8	-3.0	6.4
k1750s00	58	8	104.6	0.3	104.6	0.3	101.9	0.2	-414.3	1.7	206.4	1.5
k1753s65	59	8	87.6	3.9	87.6	3.9	82.5	4.7	-64.7	1.2	-346.5	8.0
k1824s71	59	8	48.5	3.9	48.5	3.9	47.6	4.2	-17.1	14.3	-188.3	13.2
k1828s48	32	8	78.4	6.2	47.5	5.6	78.4	6.2	171.6	8.5	58.5	2.6
k1840s56	42	8	-999.9	-999.9	60.2	7.3	20.0	1.7	-90.6	13.6	-167.4	13.3
k1928s43	46	8	31.4	0.6	31.4	0.6	31.4	0.6	66.7	5.5	-283.9	8.0
k1936s55	40	8	43.3	0.7	43.3	0.7	42.9	0.7	201.6	1.2	-307.0	7.9
k1956s17	36	8	25.6	0.2	25.6	0.2	35.9	2.0	0.8	8.6	-47.6	1.1
k2002s05	46	8	61.1	0.9	61.1	0.9	61.1	0.9	-113.1	8.3	-116.0	1.1
k2011s62	35	8	30.2	0.6	27.8	1.8	30.2	0.6	325.0	4.5	-393.5	1.1
k2023s59	41	8	46.9	4.0	35.6	4.7	35.5	3.3	77.9	4.5	-12.6	1.6
k2026s29	28	8	33.2	0.4	33.2	0.4	33.9	0.4	35.8	9.9	-372.1	9.7
k2041s35	25	8	29.9	0.5	29.9	0.5	38.0	4.5	31.2	3.3	-142.9	3.4
k2057s02	27	8	-999.9	-999.9	48.0	2.9	44.3	2.7	-4.9	6.1	-105.4	7.0
k2101s29	41	8	45.3	3.3	45.3	3.3	56.0	1.2	48.2	5.6	-20.7	1.1
k2102s60	44	8	65.4	0.8	53.2	1.7	53.7	1.7	145.7	14.0	-567.3	12.8
k2104s10	18	8	64.0	3.0	52.1	3.2	40.5	2.4	570.1	7.4	-292.7	2.9
k2107s45	22	8	84.4	0.1	84.4	0.1	84.4	0.1	96.5	2.4	-45.0	1.2
k2130s08	22	7	54.2	3.0	65.1	4.8	66.0	4.5	371.3	3.0	-38.4	6.3
k2132s14	30	8	44.1	1.7	50.9	2.3	52.3	2.4	-89.2	3.2	-159.1	1.1
k2148s63	32	5	55.7	2.2	55.7	2.2	63.9	1.5	11.5	4.2	-96.6	1.1
k2150s75	32	8	51.3	6.5	16.4	2.5	20.4	2.4	866.6	2.8	-281.3	1.0
k2157s55	25	8	27.6	0.9	27.6	0.9	27.6	0.9	68.5	8.2	-24.3	9.9
k2158s15	25	8	30.5	0.6	30.5	0.6	31.4	0.6	40.7	3.4	-70.3	9.8
k2204s56	21	8	60.4	0.1	193.8	5.3	200.3	5.3	4.8	15.0	5.6	14.9
k2206s42	13	8	-999.9	-999.9	111.7	10.8	115.8	9.8	169.1	1.8	-147.3	1.3
k2318s13	23	8	66.6	0.7	95.8	3.6	95.8	3.6	-754.6	4.8	-230.9	2.0
k2346s59	26	8	70.5	4.7	42.0	4.8	48.7	5.2	264.2	5.1	56.6	1.1
k2351s25	26	8	44.5	2.0	44.5	2.0	52.2	0.9	322.2	3.3	223.9	1.9

Next....

```
k0439s23
28 2 6 6 10 4 0 0 0 0 0 0 pr3
28 2 6 6 10 4 0 0 0 0 0 0 rr5
28 2 6 6 10 4 0 0 0 0 0 0 rwf
28 2 6 6 10 4 0 0 0 0 0 0 se2
k0443s32
6 0 1 3 2 0 5 0 2 3 0 0 pr3
6 0 1 3 2 0 5 0 2 3 0 0 rr5
6 0 1 3 2 0 5 0 2 3 0 0 rwf
6 0 1 3 2 0 5 0 2 3 0 0 se2
k0518s28
32 6 7 8 5 6 8 2 3 1 1 1 pr3
35 6 9 8 6 6 5 2 1 1 0 1 rr5
35 6 9 8 6 6 5 2 1 1 0 1 rwf
35 6 9 8 6 6 5 2 1 1 0 1 se2
k0523s14
30 0 5 7 12 6 5 0 1 4 0 0 pr3
30 0 5 7 12 6 5 0 1 4 0 0 rr5
30 0 5 7 12 6 5 0 1 4 0 0 rwf
30 0 5 7 12 6 5 0 1 4 0 0 se2
k0539s00
29 2 6 7 8 6 2 0 2 0 0 0 pr3
27 2 6 7 8 4 4 0 2 0 0 2 rr5
29 2 6 7 8 6 2 0 2 0 0 0 rwf
28 2 5 7 8 6 3 0 3 0 0 0 se2
k0559s14
40 0 12 6 18 4 8 0 2 0 6 0 pr3
37 0 11 5 18 3 11 0 3 1 6 1 rr5
38 0 11 5 18 4 10 0 3 1 6 0 rwf
41 0 12 6 19 4 7 0 2 0 5 0 se2
k0614s20
37 2 6 9 10 10 0 0 0 0 0 0 pr3
34 2 6 8 10 8 3 0 0 1 0 2 rr5
36 2 6 9 10 9 1 0 0 0 0 1 rwf
36 2 6 9 10 9 1 0 0 0 0 1 se2
k0624s45
32 0 6 10 10 6 0 0 0 0 0 0 pr3
31 0 6 9 10 6 1 0 0 1 0 0 rr5
32 0 6 10 10 6 0 0 0 0 0 0 rwf
32 0 6 10 10 6 0 0 0 0 0 0 se2
```

About 1000 frames already observed but not yet used!